Using TRMM/TMI to Retrieve Surface Soil Moisture over the Southern United States from 1998 to 2002

H. GAO AND E. F. WOOD

Department of Civil and Environmental Engineering, Princeton University, Princeton, New Jersey

T. J. JACKSON

USDA/ARS Hydrology and Remote Sensing Laboratory, Beltsville, Maryland

M. DRUSCH

European Centre for Medium-Range Weather Forecasts, Bracknell, Berkshire, United Kingdom

R. BINDLISH

USDA/ARS Hydrology and Remote Sensing Laboratory, Beltsville, Maryland

(Manuscript received 1 November 2004, in final form 21 June 2005)

ABSTRACT

Passive microwave remote sensing has been recognized as a potential method for measuring soil moisture. Combined with field observations and hydrological modeling brightness temperatures can be used to infer soil moisture states and fluxes in real time at large scales. However, operationally acquiring reliable soil moisture products from satellite observations has been hindered by three limitations: suitable low-frequency passive radiometric sensors that are sensitive to soil moisture and its changes; a retrieval model (parameterization) that provides operational estimates of soil moisture from top-of-atmosphere (TOA) microwave brightness temperature measurements at continental scales; and suitable, large-scale validation datasets. In this paper, soil moisture is retrieved across the southern United States using measurements from the Tropical Rainfall Measuring Mission (TRMM) Microwave Imager (TMI) X-band (10.65 GHz) radiometer with a land surface microwave emission model (LSMEM) developed by the authors. Surface temperatures required for the retrieval algorithm were obtained from the Variable Infiltration Capacity (VIC) hydrological model using North American Land Data Assimilation System (NLDAS) forcing data. Because of the limited information content on soil moisture in the observed brightness temperatures over regions characterized by heavy vegetation, active precipitation, snow, and frozen ground, quality control flags for the retrieved soil moisture are provided. The resulting retrieved soil moisture database will be available through the NASA Goddard Space Flight Center (GSFC) Distributed Active Archive Center (DAAC) at a 1/8° spatial resolution across the southern United States for the 5-yr period of January 1998 through December 2002. Initial comparisons with in situ observations obtained from the Oklahoma Mesonet resulted in seasonal correlation coefficients exceeding 0.7 for half of the time covered by the dataset. The dynamic range of the satellite-derived soil moisture dataset is considerably higher compared to the in situ data. The spatial pattern of the TMI soil moisture product is consistent with the corresponding precipitation fields.

1. Introduction

Soil moisture is one of the key variables for studying the terrestrial water and energy cycles because of its role in controlling the partitioning of available radiative energy into latent and sensible heat, and controlling the partitioning of precipitation into infiltration and runoff. Soil moisture integrates precipitation and evaporation over periods of days to weeks and introduces a significant element of memory in the atmosphere–land system. Soil moisture observations at large scales are critical for a variety of applications, including assimilation

Corresponding author address: Dr. Huilin Gao, School of Earth and Atmospheric Sciences, Georgia Institute of Technology, Atlanta, GA 30332.
E-mail: huilin.gao@eas.gatech.edu

© 2006 American Meteorological Society

into weather forecasting [four-dimensional data assimilation (4DDA) models], crop and drought monitoring, for initial conditions in flood forecasting, and quantifying the earth's water budget. There is strong climatological and modeling evidence that the fast recycling of water through evapotranspiration and precipitation is a primary factor in the persistence of dry or wet anomalies over large continental regions during summer (Koster and Suarez 2004). On this account, soil moisture is the most significant boundary condition that controls summer precipitation over the central United States and other large midlatitude continental regions, and has essential initial information for seasonal predictions (Koster et al. 2000, 2003, 2004; Salvucci et al. 2002).

To date there have been very few in situ soil moisture observing systems that could provide direct estimates of regional or continental soil moisture fields. Even in seemingly large networks, precise in situ measurements of soil moisture are sparse, often infrequently measured at a single point, which is only representative of a small area. The Oklahoma Mesonet system is among the largest networks; since 1996, a total number of 114 automated stations have been set up to measure soil moisture every 30 min (information available online at http://www.mesonet.org/). Robock et al. (2000) describe their global soil moisture data bank, which archives much of the available soil moisture measurements from a disperse set of networks. Soil moisture measurements at regional to continental scales could be used to address the following science questions that are central to research programs like the World Climate Research Programme (WCRP) Global Energy and Water Experiment (GEWEX), regional studies like the North American Monsoon Experiment (NAME), or agency research programs such as those in the National Aeronautics and Space Administration (NASA) related to the water cycle (information online at http://earth.nasa.gov/visions/researchstrat/):

- Is there a feedback mechanism between soil moisture and atmospheric boundary layer that can be verified?

  This has been explored somewhat by Betts (2000), Betts et al. (2003), and Berbery et al. (2003) with modeled data and assumptions, but needs observations for more definitive results.
- Do climate and weather prediction models accurately represent the land surface partitioning of precipitation into infiltration and runoff? Can they be improved by the assimilation of surface soil moisture observations?

  The North American Land Data Assimilation System (NLDAS) (Mitchell et al. 2004) has evaluated how well land surface models compare to observed soil moisture (Robock et al. 2003), while Berbery et al. (2003) has investigated the relationship between soil moisture and atmospheric processes from the coupled Eta Model.
- Can spatial and temporal surface soil moisture observations provide new information on soil hydrological processes and properties?

  Investigations have used soil moisture data to estimate soil properties (Hollenbeck et al. 1996), hydrologic processes (Jackson 2002; Salvucci 2001; Saleem and Salvucci 2002), and land–atmospheric coupling (Betts 2000). To date, scientific investigations related to these questions have often relied on model-based soil moisture fields, or on limited in situ data.

For remote sensing of soil moisture, microwave frequencies have some distinctive advantages over other spectral regions (Schmugge et al. 2002). Microwave emission at frequencies below about 10 GHz can penetrate through grass and short crops, and is essentially unaffected by atmospheric water vapor. Also, the top-of-atmosphere (TOA) microwave brightness temperature measurement is independent of sun illumination. Soil moisture can be retrieved from the microwave brightness temperature (T_B) because of the strong relationship between T_B and wet soil emissivity—increased soil moisture leads to a decrease in soil emissivity and consequently to observed brightness temperature. The sensitivity of the relationship is frequency dependent—the lower the frequency, the higher the sensitivity to soil moisture. Lower frequencies are also less affected by vegetation and surface roughness. Within the same frequency, horizontally polarized emission is more sensitive to soil wetness as compared to the vertical component.

It has been shown that low-frequency passive microwave data have the potential to improve operationally produced soil moisture fields from numerical weather prediction models (e.g., Drusch et al. 2004; Seuffert et al. 2004). The challenge is whether such remotely sensed soil moisture datasets can be achieved with sufficient accuracy and reliability from space on the continental scale for observation periods exceeding typical field experiments. For the Tropical Rainfall Measuring Mission (TRMM) Microwave Imager (TMI), the sensor characteristics include a dual-polarized passive radiometer for a frequency of 10.65 GHz, with a spatial resolution of 38 km, that measures microwave emissions over the top ~0.5 cm surface depth. The TMI has been in operation since December 1997, and its 10.65-GHz (X band) radiometer is better than previous instruments in terms of radiometric frequency, repeat cover-

age (where available), and resolution (38 km). Before TMI, low-frequency passive microwave spaceborne sensors included a 1.4-GHz (L band) sensor with a 110-km footprint on Skylab (Jackson et al. 2004), and a 6.63-GHz (C band) sensor with a 159-km footprint on the Scanning Multichannel Microwave Radiometer (SMMR), from October 1978 to August 1987. More recently, the lowest frequency available radiometric measurement was at 19.3 GHz from the Special Sensor Microwave Imager (SSM/I), which has been a part of the U.S. Defense Meteorological Satellite Program (DMSP) since 1987. Currently, the Earth Observing System (EOS) *Aqua* satellite, launched in May 2002, has both 6.9- and 10.65-GHz channels as part of its Advanced Microwave Scanning Radiometer-EOS (AMSR-E), but severe radio frequency interference (RFI) at 6.9 GHz has been detected, leaving its 10.65 GHz and TMI as the only readily available, low-frequency microwave instruments.

This paper presents a 5-yr retrieval (January 1998 through December 2002) of soil moisture from the TRMM Microwave Imager 10.65-GHz band sensor. It is our expectation that this dataset, with its accompanying data quality flags, will provide a unique dataset for the research community in addressing the above, and similar, science questions. Furthermore, this dataset will assist in evaluating retrieved soil moisture from AMSR-E.

Section 2 of the paper discusses the retrieval approach used in the study, and it utilizes the Land Surface Microwave Emission Model (LSMEM) of Drusch et al. (1999). The results of the retrievals are presented in section 3, with fields of soil moisture across the southern United States between 25° and 38°N latitude for each TMI orbit. Because of the swath width of the TMI sensor, complete coverage is not provided on each orbit, and because of the TRMM orbit characteristics, the overpass time and time between overpasses varies for a particular location. In fact, because this portion of the United States is near the top of the TRMM orbit, locations are observed with a different number of times during a 24-h period. Thus, we also provide a daily soil moisture field where the retrieved soil moisture from each orbit (with precipitated areas masked out) is averaged. Section 4 discusses sources of uncertainty in the retrieved soil moisture, and conditions under which retrievals are not possible. Within the database these are indicated by a series of quality control masks. The soil moisture dataset is to be available through NASA Goddard Space Flight Center (GSFC) Distributed Active Archive Center (DAAC).

2. Methodology and data sources

Despite comprehensive laboratory measurements and field experiments, knowledge of retrieval model parameters (e.g., fractional vegetation cover, vegetation water content) and inputs on the continental scale are incomplete. Problems associated with collecting these parameters and inputs include the following: (i) Vegetation parameters vary significantly with classification and season. In contrast, available measurements were obtained from field experiments and are limited to only a few vegetation types (Jackson and Schmugge 1991). (ii) Satellite sensor resolution is large compared to the heterogeneity in the landscape. Nonlinear scaling results in the need for "effective parameters" values rather than measured physical values. (iii) Ancillary data, specifically a source of surface temperature information, as required for retrievals from single-channel and single-polarization microwave sensors, are incomplete. Although remotely sensed infrared techniques offer a sufficiently accurate source of surface temperature data at a variety of resolutions, surface temperature products are only available under cloud-free conditions, while microwave soil moisture retrievals are possible and desirable under cloudy conditions. In this section, we review the retrieval algorithm used in this study and introduce required data sources.

a. Land Surface Microwave Emission Model

The retrieval algorithm is based on a semiempirical model for passive microwave brightness temperatures observed at the TOA as proposed by Kerr and Njoku (1990). The LSMEM comprises a set of alternative parameterizations for the key components, for example, the dielectric constant of the soil, surface roughness, or vegetation opacity (Drusch et al. 1999). A detailed description of the actual model configuration and the components used for the TMI soil retrieval presented in this study can be found in Gao et al. (2004). Beginning with an initial estimation of soil moisture, the LSMEM iteratively searches for the soil moisture value that matches the observed brightness temperature best (Gao et al. 2004). In the LSMEM formulation, the total brightness temperature ($T_{b,p}$) is a weighted average of radiation originating from bare soil ($T_{\mathrm{bs},p}$) and from vegetation covered soils ($T_{\mathrm{bv},p}$):

$$T_{\mathrm{bv},p} = T_{\mathrm{au}} + e^{-\tau_{\mathrm{at}}}(T_{\mathrm{ad}} + T_{\mathrm{sky}}e^{-\tau_{\mathrm{at}}})(1 - \varepsilon_p)e^{-2\tau^*} + e^{-\tau_{\mathrm{at}}}\{\varepsilon_p T_s e^{-\tau^*} + T_{\upsilon}(1 - \omega^*)(1 - e^{-\tau^*}) \times [1 + (1 - \varepsilon_p)e^{-\tau^*}]\}, \quad (1)$$

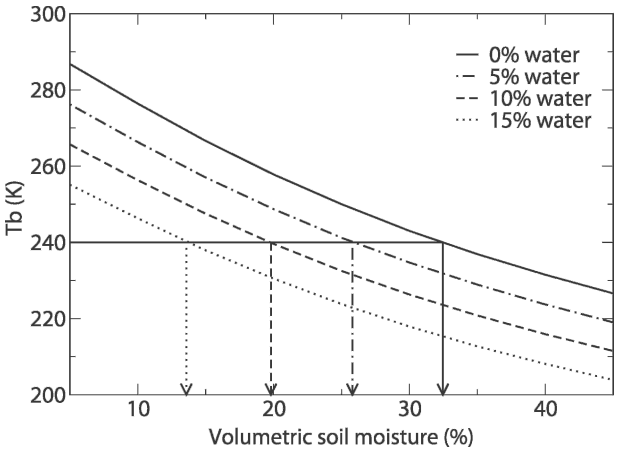

FIG. 1. The LSMEM output sensitivity to water fraction at the surface temperature of 288 K.

$$T_{\mathrm{bs},p} = T_{\mathrm{au}} + e^{-\tau_{\mathrm{at}}}(T_{\mathrm{ad}} + T_{\mathrm{sky}}e^{-\tau_{\mathrm{at}}})(1 - \varepsilon_p) + e^{-\tau_{\mathrm{at}}}\varepsilon_p T_s, \quad (2)$$

$$T_{b,p} = (1 - C_v)T_{\mathrm{bs},p} + C_v T_{\mathrm{bv},p}. \quad (3)$$

In these equations, T_{au} and T_{ad} denote the upward and downward contributions from the atmosphere, T_s the soil temperature, T_v the vegetation temperature, T_{sky} the cosmic radiation, ε_p the rough soil emissivity, and ω^* the vegetation single scattering albedo, τ_{at} and τ^* represent the optical depth of the atmosphere and the effective optical depth of the vegetation, respectively, and C_v is the fractional vegetation coverage. Subscript p indicates polarization dependency in the model representation.

For continental applications, open water has to be included. The brightness temperature of water ($T_{\mathrm{bw},p}$) is computed using Eq. (4) with $\varepsilon_{w,p}$ being the water emissivity and T_w the water temperature. As a result, the simulated TOA brightness temperature has been computed from

$$T_{\mathrm{bw},p} = T_{\mathrm{au}} + e^{-\tau_{\mathrm{at}}}(T_{\mathrm{ad}} + T_{\mathrm{sky}}e^{-\tau_{\mathrm{at}}})(1 - \varepsilon_{w,p}) + e^{-\tau_{\mathrm{at}}}\varepsilon_{w,p} T_w, \quad (4)$$

$$T_{b,p} = (1 - C_v - C_w)T_{bs,p} + C_v T_{bv,p} + C_w T_{bw,p}, \quad (5)$$

with C_W as the fractional coverage of water. A sensitivity test was carried out to simulate the brightness temperatures for footprints characterized by different water fractions and soil moisture conditions. Figure 1 shows the decrease in microwave brightness temperature as the fraction of surface water within a footprint increases. A decrease is expected because the horizontally polarized water emissivity ($\varepsilon_{w,h}$) can be well below 0.5, while soil emissivity (ε_h) at X band normally ranges from 0.85 to 0.95. These results demonstrate that the microwave emission contributions from water bodies must be taken into account in order not to overestimate volumetric soil moisture.

b. LSMEM resolution and inputs

The −3 dB footprint for TMI at X band is ~38 km over the southern United States, with an oversampling rate that results in adjacent footprint centers, which are approximately 8–13 km apart, depending on the location within the swath and the orbit. Because the supporting database from the NLDAS project (Mitchell et al. 2004) is produced at 1/8° spatial resolution, the TMI brightness temperatures have been resampled to the NLDAS grid using the nearest-neighbor technique. Because of the oversampling, interpolation would reduce the observed spatial variability. The LSMEM model inputs are listed in Table 1. All parameters and variables have been resampled to the NLDAS grid. Figure 2 shows some input fields across the United States, with Fig. 2h displaying one TMI overpass. The most relevant geophysical input parameters are discussed in the following paragraphs.

1) TMI X-BAND BRIGHTNESS TEMPERATURE

The TRMM satellite was launched in November 1997. One of the instruments on the satellite is TMI, a dual-polarization passive microwave conical scanning radiometer with an incidence angle of 52.8°, which operates at 10.65, 19.4, 21.3, and 85.5 GHz. In this study, the 10.65-GHz horizontally polarized brightness temperature has been used to retrieve soil moisture. The TRMM orbit and sensor swath result in spatial coverage between ±38° latitudes. For each day, about five orbits overpass the southern United States at various times (Bindlish et al. 2003).

2) ATMOSPHERIC CONTRIBUTIONS

At X band, the atmospheric contributions (optical depth and atmospheric emission) are comparably small with low temporal variability (Drusch et al. 2001). Consequently, it is sufficient to apply a constant atmospheric correction for the soil moisture retrieval presented in this study. A set of 3472 atmospheric temperature and humidity profiles acquired from the National Centers for Environmental Prediction (NCEP) Eta Model Output Location Time Series (MOLTS) dataset have been analyzed. They were collected at 56 sites within Oklahoma (from 34° to 38°N in

TABLE 1. LSMEM inputs.

Input class	Parameter/variable	Value	Data source	Reference
Sensor information	Incident angle	52.8°	Jackson and Hsu (2001)	
	Modeling frequency	10.65 GHz		
TMI observation	Horizontal T_b	Orbit data	U.S. Department of Agriculture	Bindlish et al. (2003)
Atmospheric contribution	Optical depth	0.014	MOLTS/radiative transfer	Drusch et al. (2001)
	Emitted T_b	6.0 K		
Surface parameters	Sand fraction, clay fraction, and soil bulk density	Spatially distributed constants	STATSGO	Miller and White (1998)
	Soil surface roughness	0.3	Choudhury et al. (1979)	
	Vegetation coverage	Spatially distributed, monthly	NLDAS greenness fraction (based on NDVI)	Chang and Wetzel (1991)
	Vegetation water content	Spatially distributed, monthly	Calculated results based on MODIS LAI and land cover types	Rodell et al. (2005)
	Water coverage	Spatially distributed constants	MODIS classification	Hansen et al. (2000)
	Vegetation structure parameter	Constants based on classification	Jackson and Schmugge (1991)	
	Vegetation single scattering albedo	0.07	Average value according to Pampaloni and Paloscia (1986), Ulaby et al. (1983)	
State variable	Surface temperature	Spatially distributed, hourly	NLDAS/VIC output	Liang et al. (1994, 1999)

latitude and from −97° to −98.5W° in longitude) during July 1999. This region and period were used because of the large number of available MOLTS data and because of the generally highly variable summertime humidity for which the atmospheric affects would be most noticeable. For each of the profiles, the optical depth and the brightness temperature of the atmosphere were calculated at 10.65, 19.35, and 22.235 GHz based on the gas absorption scheme described in Drusch et al. (2001). Averaged values for T_{ad} and T_{au} from this dataset were used as LSMEM inputs for the TMI retrieval.

3) SURFACE ROUGHNESS PARAMETER

For this parameter there is no robust data source over large spatial domains. A constant value of 0.3, which is typical for a medium rough surface, was selected (Choudhury et al. 1979). The constant value does not take into account the fact that h should scale with wavelength (Choudhury et al. 1979) and vary with surface type. However, setting a constant value is the most widely used approach for accounting for the effects of surface roughness on the modeled brightness temperatures (Drusch et al. 2004). A sensitivity test over a rangeland land cover shows that 10% uncertainty in surface roughness will result in an error of about 3% volumetric soil moisture.

4) VEGETATION STRUCTURE PARAMETER AND VEGETATION SINGLE SCATTERING ALBEDO

The effective optical depth of the vegetation (τ^*) in Eq. (1) is the product of the vegetation structure parameter (b) and vegetation water content (W_c) (Jackson and Schmugge 1991). The b parameter is a function of the canopy type/structure, polarization, and wavelength. However, studies in the literature on these dependencies are far from being complete. An approximate parameterization over the United States was made for the current investigation by assigning b values to different vegetation classes according to Table 1 in Jackson and Schmugge (1991). For vegetation types without available b values (forest, woodland, and shrub), the value of 0.7 at X band was assigned based upon Fig. 4 in Jackson and Schmugge (1991).

In Eq. (1), the soil emission from below the canopy is affected by the vegetation single scattering albedo (ω^*). According to the literature (Pampaloni and Paloscia 1986; Ulaby et al. 1983), ω^* varies from 0.04 to 1.0. An average value of 0.07, which is assumed to be polarization independent, was used for LSMEM input.

5) WATER FRACTIONAL COVERAGE

Figure 3 shows the statistics of fractional water coverage for NLDAS grid boxes within our study area. It has been derived from the NLDAS land cover data-

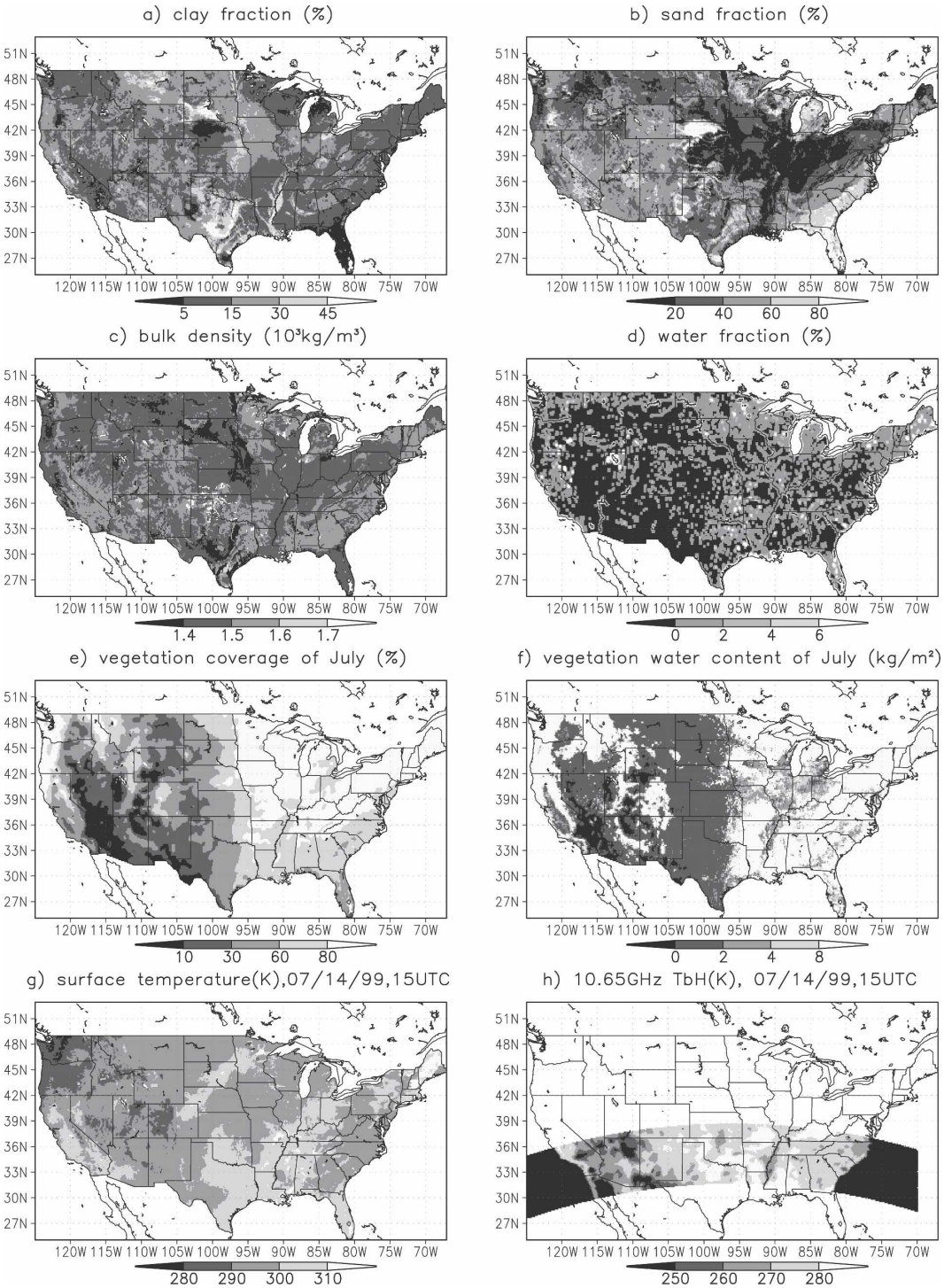

FIG. 2. Examples of LSMEM data and inputs.

base, which draws from the 1-km Moderate Resolution Imaging Spectroradiometer (MODIS) land cover data developed at the University of Maryland (Hansen et al. 2000). These data were then reprocessed so that the grid box value represents the water fraction of a TMI X-band footprint. Although most areas have less than 1% water coverage, 11% of the total number of grid boxes has a substantial water fraction of more than 5%. According to Fig. 1, if the microwave emissions from water bodies are ignored for grid boxes with 5% frac-

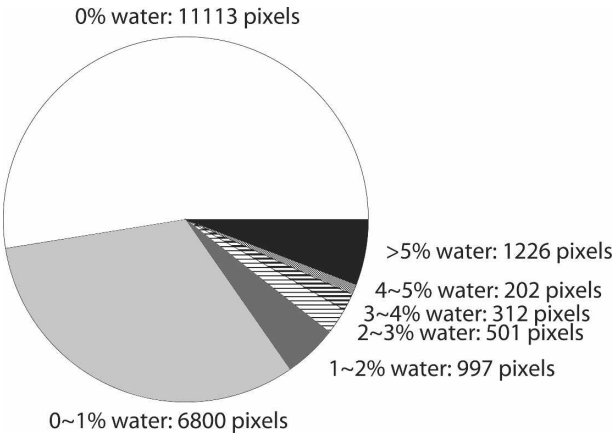

FIG. 3. Fractional area covered by water for the grid boxes within the study area.

tional water, then the overestimation of the retrieved soil moisture will be approximately 5%. Figure 2d shows the fraction as a spatial map across the United States.

6) SOIL TEXTURE

Soil texture information (sand fraction, clay fraction, and bulk density) is required for calculating the dielectric constant of wet soils. These data are obtained from the State Soil Geographic (STATSGO) database (Miller and White 1998) and were resampled to the 1/8° grid. Both the water fraction and the soil parameters (see Figs. 2a–d) are spatially heterogeneous but invariant with time.

7) VEGETATION FRACTIONAL COVERAGE AND VEGETATION WATER CONTENT

The monthly vegetation fractional coverage is available from the NLDAS database, and was calculated from the normalized difference vegetation index (NDVI) using (Chang and Wetzel 1991)

$$f_{\mathrm{veg}} = \begin{cases} 1.5(\mathrm{NDVI} - 0.1) & \mathrm{NDVI} \leq 0.547 \\ 3.2(\mathrm{NDVI} - 1.08) & \mathrm{NDVI} > 0.547. \end{cases} \quad (6)$$

One example of vegetation fractional coverage is plotted in Fig. 2e.

Vegetation water content (W_c), which contributes to vegetation optical depth (τ^*), was derived from the land cover classification and monthly leaf area index (LAI), using MODIS C-4 LAI available through Boston University. The vegetation water content was computed using general relationships between LAI, foliar and stem biomass, and estimates of their relative water content (Rodell et al. 2005). The vegetation water content for July is shown in Fig. 2f.

8) SURFACE TEMPERATURE

As explained in the introduction to section 2, the retrieval algorithm used in this paper is based on a single-frequency single polarization. Thus, physical surface temperatures are required. To avoid the constraints of only clear-sky retrievals (i.e., if surface temperatures derived from infrared measurements would be used), the surface temperatures that will be used for the retrieval are based on the Variable Infiltration Capacity (VIC) land surface scheme (Liang et al. 1994, 1999). Mitchell et al. (2004) provides a comparison among NLDAS modeled surface temperatures, estimates based on the Geostationary Operational Environmental Satellite (GOES), and instruments deployed as part of the Atmospheric Radiation Measurement (ARM) Cloud and Radiation Test Bed (CART) facility in the Southern Great Plains region of the United States. This comparison showed absolute bias between the models and the GOES or ARM CART data in the range of 0.3–6.5 K and an rms difference of around 3.5 K. For VIC, the absolute bias ranged from 0.5 to 2.8 K, depending on the season, and the rms of the difference ranged from 3.3 to 4.3 K. A sensitivity test over rangeland land cover shows that 1-K error in surface temperature results in an error of about 1% in the retrieved volumetric soil moisture. The NLDAS system is run hourly and the surface temperature that matched the TMI overpass times was used in the retrievals for both the soil temperature and vegetation temperature because the VIC LSM only has a single surface layer (see Fig. 2g for an example field).

3. Results

a. Surface soil moisture retrieved for each TMI orbit

Using the LSMEM and the parameters and inputs described in section 2, soil moisture fields were retrieved on an orbit overpass basis from 1 January 1998 through 31 December 2002. As described earlier, up to five overpasses may occur over the southern United States on any particular day. Although the overpass time varies during the day, the patterns and retrieved soil moisture values from the different orbits are consistent. Data quality masks, which help to indicate locations where we have low confidence in the retrieved product, will be discussed in section 4.

b. Daily surface soil moisture composites

For many hydrological applications (e.g., providing initial conditions for streamflow forecasting, crop moni-

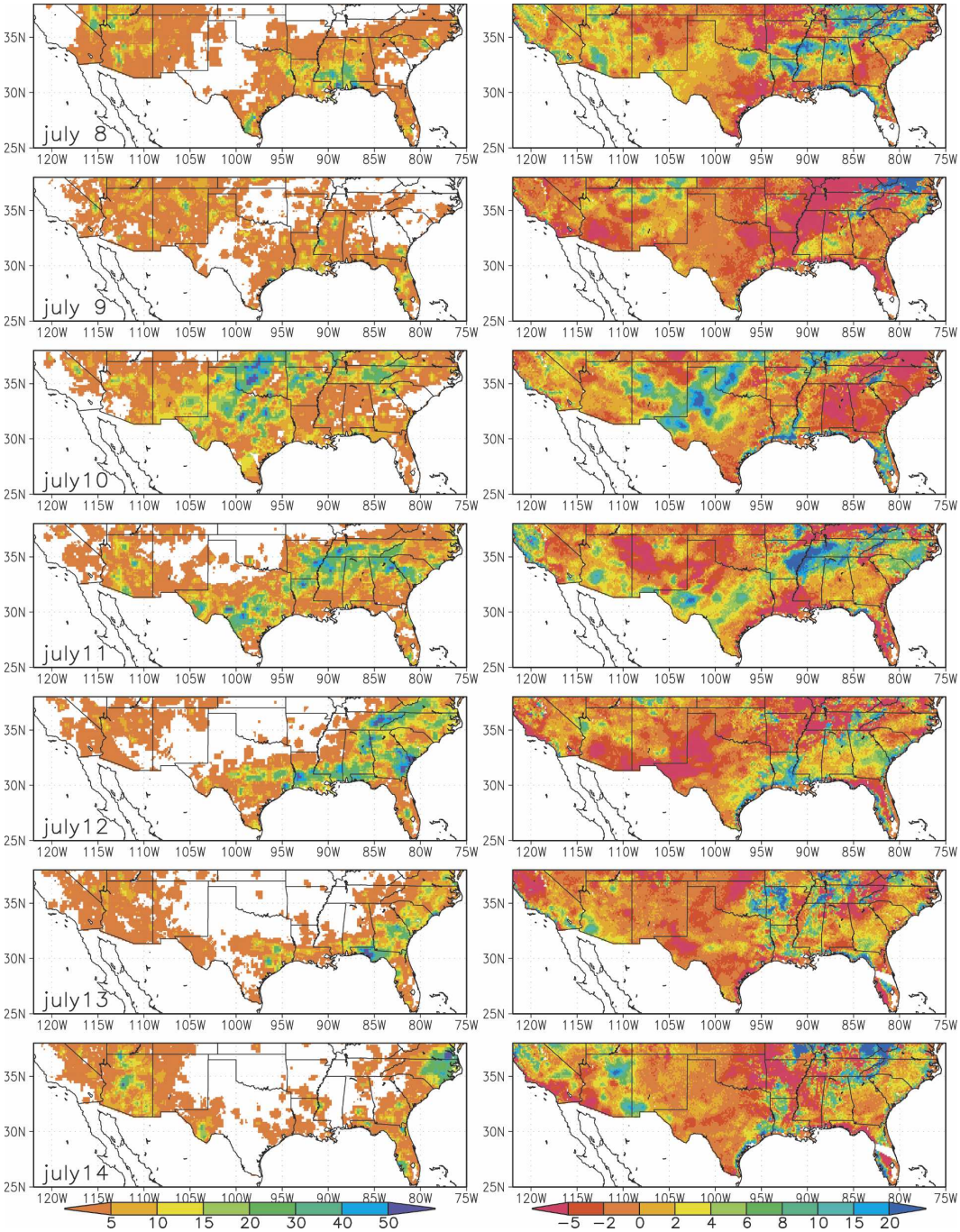

FIG. 4. (left) Daily total precipitation (mm) and (right) the second-day soil moisture increment (%) from 8 to 14 Jul 1999.

toring, etc.) soil moisture information is needed on a daily basis. Because the TRMM orbits cover different portions of the study area, a daily composite was made by combining the retrieved soil moisture values from all of the overpasses occurring during a day. When multiple overpasses occurred for a grid box, its daily average was computed from the multiple retrieved values.

Figure 4 presents a 1-week period (8 July to 14 July 1999) of the daily change in estimated soil moisture ($\text{day}_n - \text{day}_{n-1}$) compared to the daily precipitation from NLDAS forcing during day_{n-1}. The main conclusions from this comparison are as follows: 1) the soil moisture changes are hydrologically consistent with the precipitation in most areas, except for portions of the

southeastern United States; 2) the soil moisture drydown in areas without precipitation is clearly evident; and 3) the effects of large-scale irrigation can be seen in areas like the central valley in California, where high values of soil moisture are observed, without rainfall occurring.

4. Quality control masks

We recognize that there are conditions under which soil moisture cannot be accurately retrieved because of the X-band sensor sensitivity, weather conditions, or surface features. In this section, these error sources are analyzed and masks are developed for quality control. This allows the users of the dataset to access the final soil moisture product and to apply the quality control masks.

a. Precipitation mask

At X band, the sensor-observed brightness temperature is affected by falling precipitation (liquid or solid) (Tsang et al. 1977). To avoid the complex impact of falling precipitation, retrievals for grid boxes where it is precipitating were removed using hourly stage IV precipitation data from the NLDAS data system. The mask uses a 1-mm threshold for the hour of the satellite overpass to determine whether it was precipitating. This mask is applied to the orbit retrievals.

b. Vegetation sensitivity mask

In analyzing the retrieved soil moisture, we noted that in some regions, particularly in the southeastern United States, the soil moisture dynamics are not consistent with the precipitation dynamics. Specifically, most of these areas have consistently low soil moisture values (less than 10% most of the time) with little variability. These results warranted further investigation.

To do the analysis, the 10.65-GHz polarization ratio ($T_{b,V}/T_{b,H}$) was studied. This ratio is almost independent of surface temperature and thus its soil moisture sensitivity mainly depends on land cover conditions. The monthly average of the ratio for July 1999 is plotted in Fig. 5a and the standard deviation is presented in Fig. 5b. These images indicate that the polarization ratios for the "consistently dry" areas in Fig. 5 are low (high $T_{b,H}$) and vary slightly. The low variability confirms that the dynamics of the precipitation (and of the subsequent soil moisture) is not being captured in the brightness temperatures or polarization ratio, and thus the soil moisture cannot be retrieved accurately.

A comparison between the above areas and a vegetation classification shows that the areas of low polarization sensitivity and dynamics are over forested regions. In forested regions the vegetation optical depth is large, and causes a high TOA brightness temperature with little polarization (Ulaby et al. 1986). Consequently, over the forests, the soil microwave 10.7-GHz emission cannot penetrate the canopy and the vegetation brightness temperatures that are observed by the satellite sensor are high resulting from the high emissivity of the forest canopy (Ulaby et al. 1986). In the absence of vegetation information, the retrieval model would estimate consistently low soil moisture from the constantly high observed brightness temperature. A reasonable consistency is also observed between the polarization pattern (Fig. 5a) and the vegetation water content map (Fig. 2f). Accordingly, it is our assessment that soil moisture retrievals for areas with heavy vegetation are not reliable and should be masked out. As an aside, the emission from heavy vegetation also suggests that subgrid-, small-scale patches of large trees, if ignored as is the usual practice, will tend to increase the average brightness temperature in a scene resulting in a

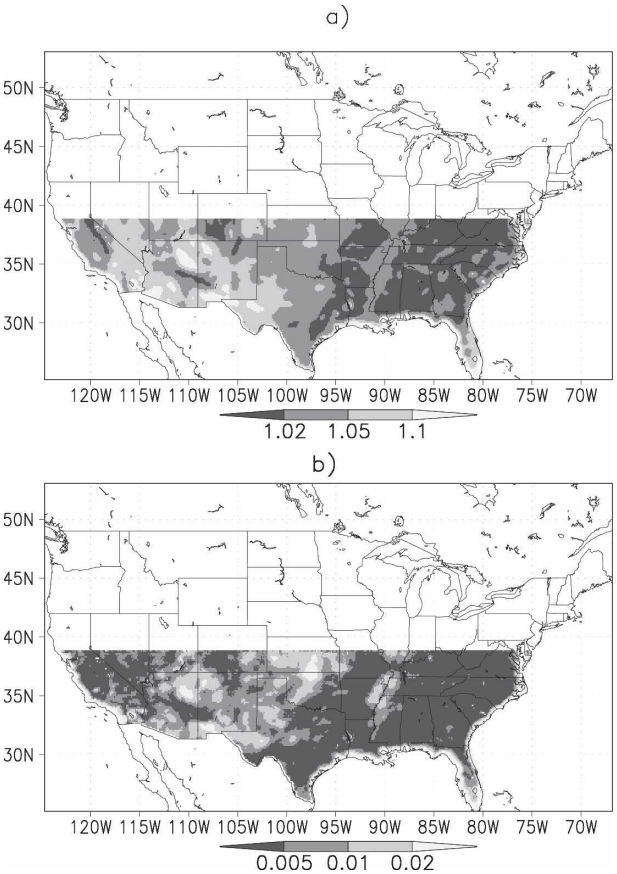

FIG. 5. TMI 10.7-GHz polarization ratio for Jul 1999 over the southern United States: (a) monthly average $T_{b,V}/T_{b,H}$ and (b) a monthly standard deviation of $T_{b,V}/T_{b,H}$.

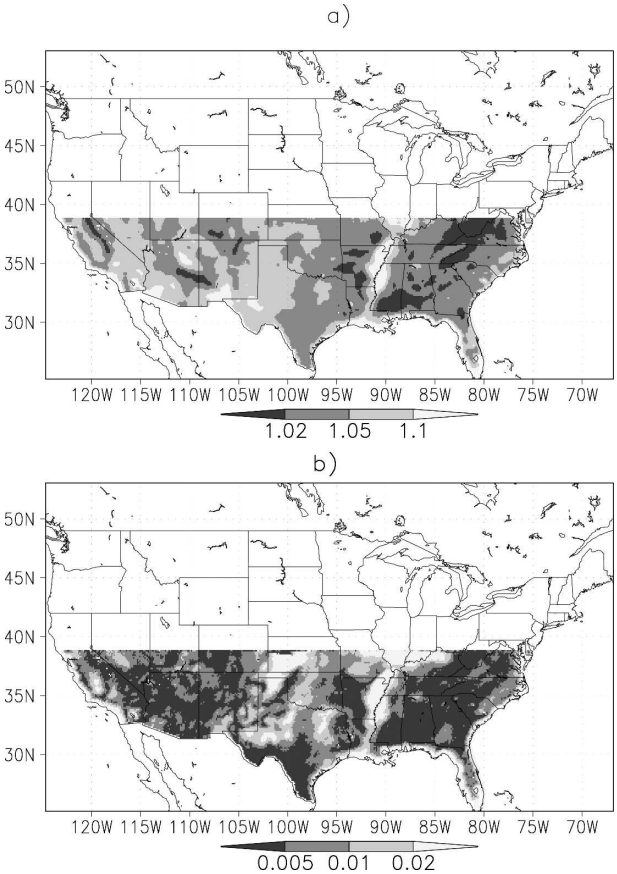

FIG. 6. As in Fig. 5 but for Jan 1999.

lower mean retrieved surface moisture. This may explain part of the differences between the mean retrieved soil moisture and observation (shown in Fig. 10).

Because vegetation mass varies seasonally, the polarization ratio sensitivity analysis was computed for each month. The results for January 1999 are shown in Fig. 6, and a comparison of Figs. 5a and 6a shows an expanded area with potentially good retrievals in January when compared to July. We have used a monthly averaged polarization ratio of below 1.02 and a standard deviation less than 0.005 to determine areas where we feel the vegetation effects prevent reliable retrievals.

c. *Snow cover, frozen soil, and surface water contamination mask*

The current version of the LSMEM does not consider the emission from snow-covered or frozen soil, and cannot be used to retrieve soil moisture under these conditions. Basically, when the soil is frozen the algorithm for calculating wet soil dielectric constant no longer holds. Thus, a daily frozen soil and snow cover classification dataset, provided by the National Snow and Ice Data Center (NSIDC) (Zhang et al. 2003), was reprocessed to the NLDAS 1/8° grid and used as the mask. This dataset, based on processing SSM/I data, also identifies coastal areas (including those of large lakes) where water contamination degrades any retrievals. These areas are masked out in our TMI dataset. Figure 7 presents an image of the snow-, frozen soil–, and water-contaminated areas for 1 January 1999.

d. *Data availability*

Figure 8 presents an example (for 1 January 1999) of the retrieved soil moisture with all areas screened out where the retrievals are suspect. To provide a synoptic description of the data availability over the 5 yr, Fig. 9

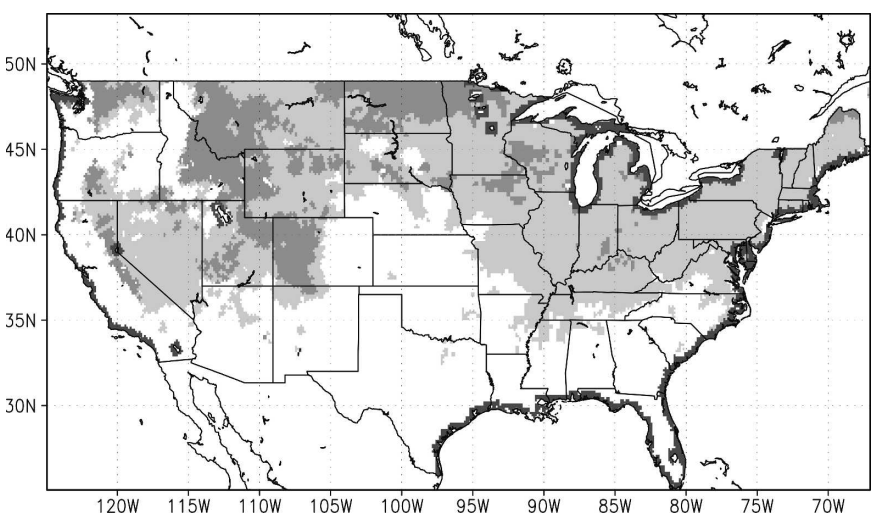

FIG. 7. Mask for frozen ground (bright gray), snow cover (gray), and water contamination (dark gray).

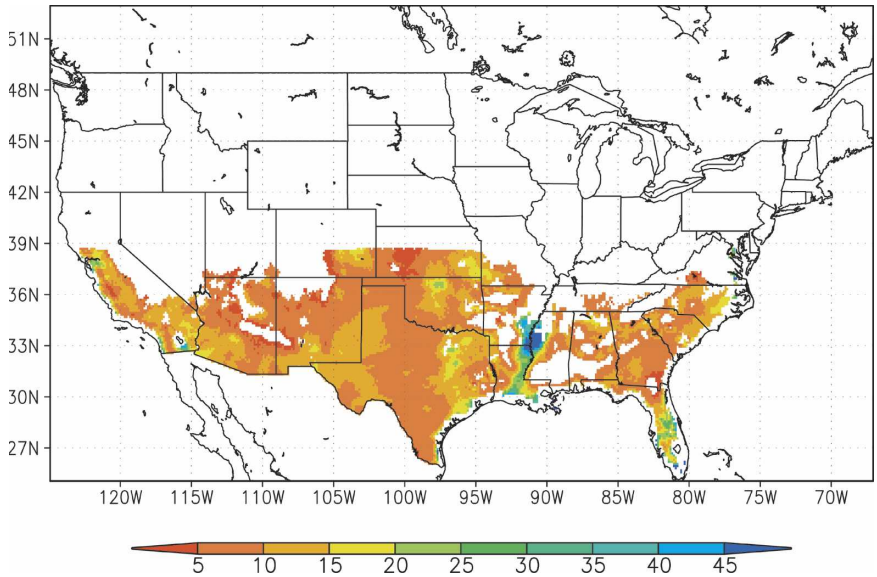

FIG. 8. Retrieved surface volumetric soil moisture (%) for 1 Jan 1999 with all quality masks applied.

presents the percentage of days within a season when the retrieved soil moisture passed all quality flags. In the summer, the major factor influencing the retrieved soil moisture is heavy vegetation; in the winter, the major factor is snow cover and frozen soil. A full description of the available data product is presented in the appendix.

5. Initial comparisons with Oklahoma Mesonet in situ measurements

Historically the "validation" of remote sensing products consisted of comparisons to ground-based measurements with the goal of having the former match the latter. This approach to validation needs to be revised, because too often the ground-based observations are taken at different spatial and temporal scales than the remote sensing measurements rendering them inappropriate for direct comparison. Nonetheless, it seemed appropriate that some comparisons to in situ be provided here.

The Oklahoma Mesonet (information online at http://www.mesonet.org) is an operational environmental monitoring network that consists of 114 stations, with at least one in each of the 77 Oklahoma counties. From 1998, soil moisture point values at 72 stations at depths of 5, 25, 60, and 75 cm are available. The volumetric soil moisture is estimated using a calibrated change in soil temperature over time after a heat pulse is introduced (heat dissipation sensor).

Figure 10 presents the Oklahoma Mesonet– and TMI-retrieved soil moisture for the period of June–October 2002, with Fig. 10a comparing the retrieved soil moisture from the El Reno Mesonet site with the corresponding grid box and Fig. 10b comparing the average "Mesonet-wide" soil moisture from the reporting sites with the average TMI soil moisture of the grid boxes overlaying those sites. Also shown is the El Reno (Fig. 10a) or Mesonet average (Fig. 10b) daily precipitation values. Qualitatively, the comparison show the following: 1) in general at both scales, TMI and the Oklahoma Mesonet soil moisture show good responses to precipitation, while there are a couple of rainfall events captured by TMI but not in the Mesonet site at El Reno, for example, rainfall at the end of June and around 20 July; 2) TMI-retrieved soil moisture has a lower mean value and larger dynamic range and a faster dry-down, which can be attributed to its shallower (~0.5 cm) sensing depth as compared to the Mesonet 5-cm depth; and 3) the El Reno data show that the sensor appears to have a lower bound on reported soil moisture of about 22%, and that moisture saturation occurs in the Mesonet but not in the TMI-retrieved values.

The daily average of the 72 Mesonet sites and TMI data for the grid overlaying the Mesonet site was computed to obtain a Mesonet-wide daily average soil moisture value. This provides a regional daily soil moisture estimate that should be more consistent with the observing scale of TMI. Basically, the comparison between the Mesonet-wide and TMI soil moisture time series displays the same characteristics as the comparison for El Reno, except that the time series are "damped," resulting from the averaging of the 72 sites.

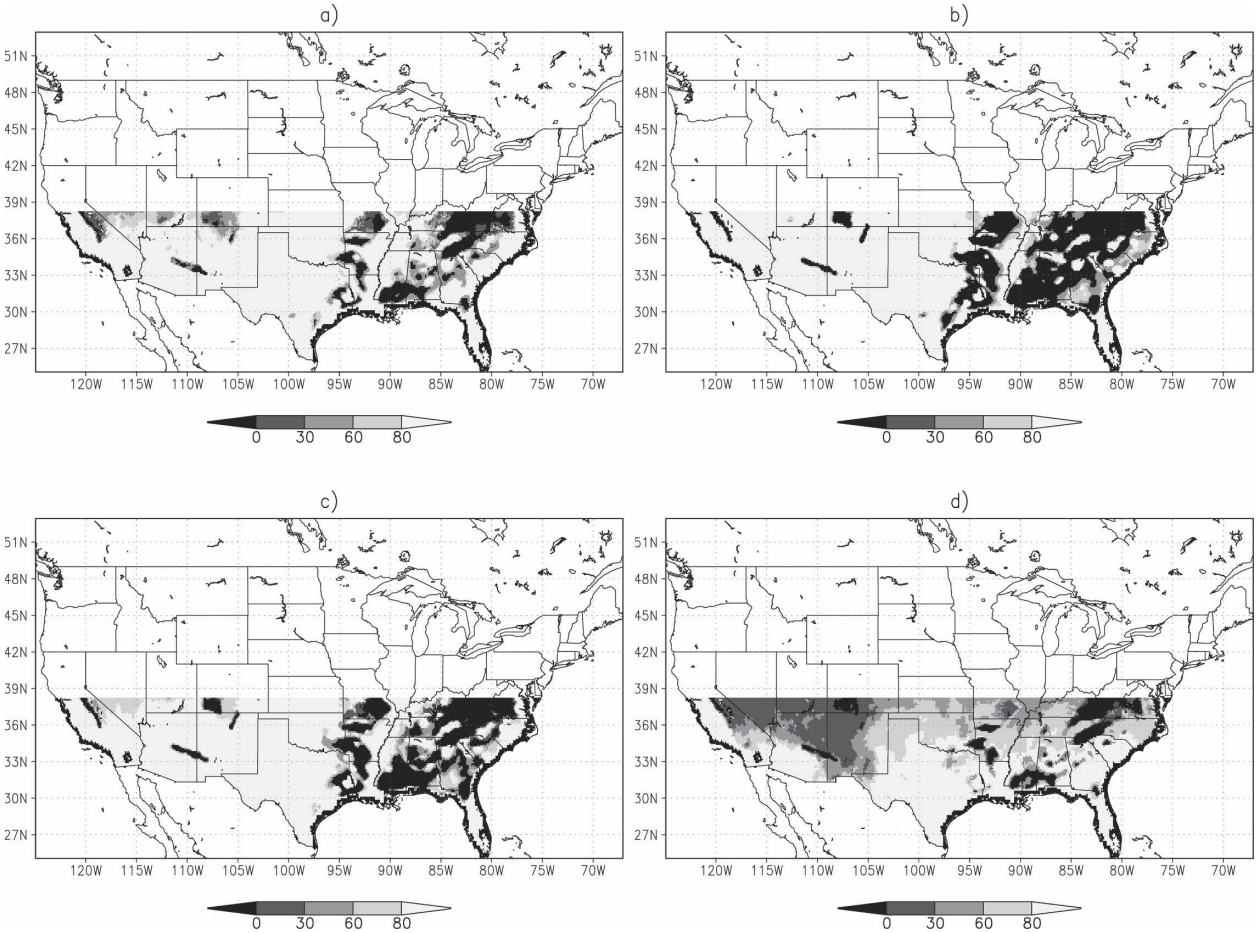

FIG. 9. Percentage of time by season that the retrieved soil moisture passed all data quality flags: (a) MAM, (b) JJA, (c) SON, and (d) DJF.

Table 2 provides for each year and over the 5-yr dataset seasonal statistics for both the Mesonet-wide average (OK_M) and the TMI-averaged (TMI) soil moisture time series. These statistics include means, coefficients of variation, and correlation between OK_M and TMI. Table 2 confirms the low variability in the Oklahoma Mesonet data, whose seasonal coefficients of variation varies from a low of 0.018 in the December–January–February (DJF) season to a high of 0.045 in June–July–August (JJA), with March–April–May (MAM) being 0.030 and September–October–November (SON) being 0.040. For TMI these corresponding seasonal statistics are 0.15 (DJF), 0.20 (MAM), 0.21 (JJA), and 0.18 (SON). The correlation between the Mesonet-wide soil moisture and TMI average shows a strong seasonal trend as well as large interannual variability. The seasonal trend has the lowest correlation in winter (0.41 for DJF) and highest in the autumn (0.74 in SON). It is encouraging that for the three nonwinter seasons, the correlations are greater than 0.50 for all years, with the autumn (SON) being higher than 0.69. This shows a remarkable correlation between the two datasets whose observing techniques and scales are so different, and between two datasets that may appear at first glance are not comparable. There is some concern regarding the large interannual variability in the correlations, which will require further investigation. In a similar manner, the correlations between the monthly soil moisture anomalies (monthly soil moisture subtracted from its monthly average from the 5 yr) were computed between TMI and Mesonet as 0.78, which confirms that at the monthly temporal scale they covary well. Similar correlations between the Mesonet monthly rainfall anomalies and Mesonet (TMI) soil moisture anomalies resulted in correlations of 0.68 (0.54), again demonstrating the good correspondence between the TMI-retrieved soil moisture and Mesonet soil moisture. From these evaluations, we conclude that the two datasets are comparable.

6. Summary

This paper describes the retrieval of soil moisture across the southern United States from TMI X-band

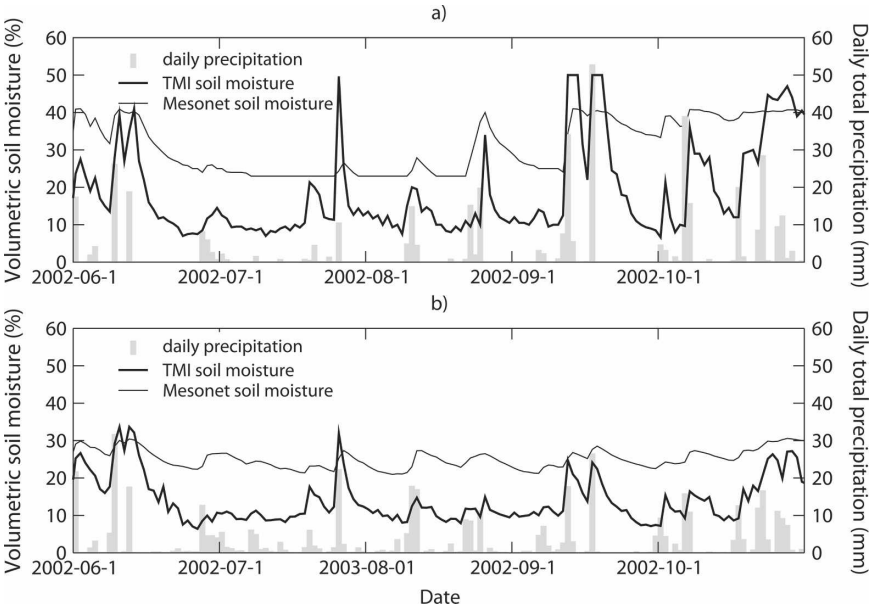

FIG. 10. Retrieved soil moisture from TMI and Oklahoma Mesonet with observed precipitation for the period of Jun through Oct 2002 for (a) the El Reno Mesonet site and (b) averaged over the 72 Oklahoma Mesonet sites reporting soil moisture.

brightness measurements using the LSMEM of Drusch et al. (1999), augmented by including microwave emissions from surface water bodies. Determining the retrieval model parameters such that quasi-operational retrievals can be obtained is important if routine estimates are to be retrieved. The paper describes the available sources of information from which these parameters can be estimated, as well as the reliability of

TABLE 2. Seasonal and annual statistics for Oklahoma Mesonet and TMI-retrieved soil moisture averaged over the 72 Mesonet sites.

	Mean soil moisture (OK_M)	Coefficient of variation (OK_M)	Mean soil moisture (TMI)	Coefficient of variation (TMI)	Correlation (OK_M, TMI)
DJF	29.4	0.018	12.2	0.15	0.41
1998	30.9	0.008	13.9	0.17	0.75
1999	29.5	0.021	11.9	0.12	0.70
2000	27.9	0.029	10.1	0.13	0.24
2001	30.9	0.010	14.1	0.20	0.24
2002	27.7	0.024	11.1	0.12	0.13
MAM	28.5	0.030	14.5	0.20	0.60
1998	27.8	0.035	14.9	0.23	0.74
1999	29.1	0.034	15.6	0.18	0.62
2000	28.6	0.032	13.5	0.18	0.48
2001	28.7	0.029	14.8	0.17	0.59
2002	28.5	0.021	13.7	0.22	0.58
JJA	24.6	0.045	11.9	0.21	0.62
1998	22.6	0.034	10.1	0.22	0.42
1999	25.5	0.047	11.4	0.21	0.86
2000	25.9	0.066	12.3	0.18	0.52
2001	23.8	0.039	11.5	0.22	0.76
2002	25.3	0.039	14.3	0.21	0.56
SON	25.5	0.040	11.9	0.18	0.74
1998	27.0	0.041	13.2	0.22	0.75
1999	24.5	0.054	9.5	0.18	0.80
2000	25.1	0.031	12.0	0.16	0.73
2001	24.9	0.038	10.5	0.14	0.69
2002	26.1	0.035	14.2	0.19	0.71

the data. For data such as soil texture, extensive databases are available for the United States. For parameters such as the soil roughness parameter or the vegetation single scattering albedo, representative values were used based on studies and field measurements reported in the literature. Some parameters and inputs, such as the land surface temperatures and atmospheric microwave contribution to the TOA measurements were derived from other models. In the case of land surface temperature, this allowed the retrieval of soil moisture under cloudy conditions when satellite IR-based estimates are unavailable. The accuracy of surface temperatures (Mitchell et al. 2004) is sufficient for their use in the soil moisture retrieval algorithm. Finally, some parameter values are calculated from other remote sensing products, such as monthly vegetation water content and monthly vegetation fractional coverage. For this investigation, all of these inputs were resampled to 1/8° grids to be consistent with the NLDAS data assimilation data system.

Using the LSMEM retrieval model, a 5-yr soil moisture dataset for each TMI orbit across the southern United States was derived, and is provided as the level 1 data product. To make the data more suitable for general applications, a level 2 product consisting of daily fields compiled using the level 1b data, with averaged soil moisture values for locations with multiple TMI overpasses. The highest quality data product is the level 3 product, in which areas of poor retrievals resulting from heavy vegetation, snow cover, frozen ground, and water contamination are masked out. In analyzing the soil moisture sensitivity over various vegetation types, we conclude that only forested regions resulted in failed retrievals, which is a better result than we initially expected.

Initial comparisons with soil moisture estimates from the Oklahoma Mesonet heat dissipation sensors, averaged across 72 Mesonet sites, shows that the retrieved TMI soil moisture product is comparable to the in situ–estimated soil moisture values, with seasonal correlations as high as 0.86, and with an average seasonal correlation of 0.59. Comparisons during DJF were poorest and SON had the best in term of overall seasonal compatibility. Though evaluating remote sensing results is rather challenging, considering the different scales, representative depths of the two datasets, the preliminary comparisons indicate the TMI retrievals to be encouraging.

The TMI X-band-retrieved soil moisture described in this paper serves as a long-term, continental-scale data product available to the community for use in weather and climate studies. Its use by the community will help address science questions central to global water and energy studies, provide experimental data to test soil moisture data assimilation systems, and explore the usefulness in water resource applications like flood forecasting and agriculture. Through such use, the community will better understand the potential uses for soil moisture products based on NASA's *Aqua*'s AMSR-E and the planned Hydrosphere State (HYDROS) L-band microwave mission.

Acknowledgments. This research was supported by NASA TMI pathfinder project (NAG5-9635) and NASA AMSR-E validation project (NAG5-11111). The authors acknowledge the availability of data from NLDAS project, of which the second author is a coinvestigator. The authors also acknowledge and appreciate the availability of MOLTS data from the NCEP Web site, the soil moisture data made available by the Oklahoma Mesonet system, the frozen soil data made available to us by Dr. T. Zhang of NSIDC, the LAI data made available by the climate and vegetation research group of Boston University, and the vegetation water content algorithms provided by Dr. J. Kimball of the University of Montana. M. Drusch was partly funded by the German Climate Research Program DEKLIM (01LD0006). This research and dataset could not have been carried out without these data and help.

APPENDIX

Available Data Products

The following retrieved soil moisture and related data quality products are being provided to the NASA GSFC DAAC:

- Level 1: Level 1 provides the retrievals for each orbit, with level 1a being the soil moisture retrieved for each TMI overpass, using the LSMEM (Gao et al. 2004), without consideration of the retrieval quality considerations discussed in section 4. Level 1b is the same as level 1a but with the precipitation masks applied. The size of each is ~1.9 GB.
- Level 2: Level 2 provides daily averaged fields using level 1b data with averaged soil moisture values for locations with multiple TMI overpasses on that day that passed the active precipitation quality flag (see section 4a). The size is ~377 MB.
- Level 3: Level 3 provides daily-averaged quality-screened fields. Level 2 data fields with areas screened out because of retrieval concerns from heavy vegetation, snow cover, and frozen soil (see sections 4b and 4c). The size is ~377 MB. The quality control data for each condition (heavy vegetation, snow cover, frozen soil, and water contamination) is

provided. The size for the each heavy vegetation masks is 207 KB, and there is one for each month. The size for the snow cover, frozen soil, and water contamination mask files is 377 MB.

The data format is binary Little-Endian, 4-bytes for each grid box, with 464 columns by 112 rows. Areas masked out have a value of 0; areas where there are no TMI retrievals have a value of $9.999 \times e^{20}$. All retrieved soil moisture values are greater than 0 so no conflict with the mask files will occur.

REFERENCES

Berbery, E. H., Y. Luo, K. E. Mitchell, A. K. Betts, 2003: Eta model estimated land surface processes and the hydrologic cycle of the Mississippi basin. *J. Geophys. Res.*, **108,** 8852, doi:10.1029/2002JD003192.

Betts, A. K., 2000: Idealized model for equilibrium boundary layer over land. *J. Hydrometeor.,* **1,** 507–523.

——, J. H. Ball, M. Bosilovich, P. Viterbo, Y. C. Zhang, W. B. Rossow, 2003: Intercomparison of water and energy budgets for five Mississippi subbasins between ECMWF reanalysis (ERA-40) and NASA Data Assimilation Office fvGCM for 1990–1999. *J. Geophys. Res.*, **108,** 8618, doi:10.1029/2002JD003127.

Bindlish, R., T. J. Jackson, E. F. Wood, H. Gao, P. Starks, D. Bosch, and V. Lakshmi, 2003: Soil moisture estimates from TRMM Microwave Imager observations over the Southern United States. *Remote Sens. Environ.,* **85,** 507–515.

Chang, J. T., and P. J. Wetzel, 1991: Effects of spatial variations of soil moisture and vegetation on the evolution of a prestorm environment: A numerical case study. *Mon. Wea. Rev.,* **119,** 1368–1390.

Choudhury, B. J., T. J. Schmugge, A. Chang, and R. W. Newton, 1979: Effect of surface roughness on the microwave emission from soils. *J. Geophys. Res.,* **84,** 5699–5706.

Drusch, M., R. Lindau, and E. F. Wood, 1999: The impact of the SSM/I antenna gain function on land surface parameter retrieval. *Geophys. Res. Lett.,* **26,** 3481–3484.

——, E. F. Wood, and T. J. Jackson, 2001: Vegetative and atmospheric corrections for soil moisture retrieval from passive microwave remote sensing data: Results from the Southern Great Plains Hydrology Experiment 1997. *J. Hydrometeor.,* **2,** 181–192.

——, ——, H. Gao, and A. Thiele, 2004: Soil moisture retrieval during the Southern Great Plains Hydrology Experiment 1999: A comparison between experimental remote sensing data and operational products. *Water Resour. Res.,* **40,** W0250410, doi:10.1029/2003WR002441.

Gao, H., E. F. Wood, M. Drusch, W. T. Crow, and T. J. Jackson, 2004: Using a microwave emission model to estimate soil moisture from ESTAR observations during SGP99. *J. Hydrometeor.,* **5,** 49–63.

Hansen, M. C., R. S. Defries, J. R. G. Townshend, and R. Sohlberg, 2000: Global land cover classification at 1 km spatial resolution using a classification tree approach. *Int. J. Remote Sens.,* **21,** 1331–1364.

Hollenbeck, K. J., T. J. Schmugge, G. M. Hornberger, and J. R. Wang, 1996: Identifying soil hydraulic heterogeneity by detection of relative change in passive microwave remote sensing observations. *Water Resour. Res.,* **32,** 139–148.

Jackson, T. J., 2002: Remote sensing of soil moisture: Implications for groundwater recharge. *Hydrogeol. J.,* **10,** 40–51.

——, and T. J. Schmugge, 1991: Vegetation effects on the microwave emission from soils. *Remote Sens. Environ.,* **36,** 203–219.

——, and A. Y. Hsu, 2001: Soil moisture and TRMM Microwave Imager relationships in the Southern Great Plains 1999 (SGP99) experiment. *IEEE Trans. Geosci. Remote Sens.,* **39,** 1632–1642.

——, ——, A. van de Griend, and J. R. Eagleman, 2004: Skylab L band microwave radiometer observations of soil moisture revisited. *Int. J. Remote Sens.,* **25,** 2585–2606.

Kerr, Y. H., and E. G. Njoku, 1990: A semiempirical model for interpreting microwave emission from semiarid land surfaces as seen from space. *IEEE Trans. Geosci. Remote Sens.,* **28,** 384–393.

Koster, R. D., and M. J. Suarez, 2004: Suggestions in the observational record of land–atmosphere feedback operating at seasonal time scales. *J. Hydrometeor.,* **5,** 567–572.

——, ——, and M. Heiser, 2000: Variance and predictability of precipitation at seasonal-to-interannual timescales. *J. Hydrometeor.,* **1,** 26–46.

——, ——, R. W. Higgins, and H. M. Van den Dool, 2003: Observational evidence that soil moisture variations affect precipitation. *Geophys. Res. Lett.,* **30,** 1241, doi:10.1029/2002GL016571.

——, and Coauthors, 2004: Regions of strong coupling between soil moisture and precipitation. *Science,* **305,** 1138–1140.

Liang, X., D. P. Lettenmaier, E. F. Wood, and S. J. Burges, 1994: A simple hydrologically based model of land-surface water and energy fluxes for general-circulation models. *J. Geophys. Res.,* **99,** 14 415–14 428.

——, E. F. Wood, and D. P. Lettenmaier, 1999: Modeling ground heat flux in land surface parameterization schemes. *J. Geophys. Res.,* **104,** 9581–9600.

Miller, D. A., and R. A. White, 1998: A conterminous United States multilayer soil characteristics dataset for regional climate and hydrology modeling. *Earth Interactions,* **2**. [Available online at http://EarthInteractions.org.]

Mitchell, K. E., and Coauthors, 2004: The multi-institution North American Land Data Assimilation System (NLDAS): Utilizing multiple GCIP products and partners in a continental distributed hydrological modeling system. *J. Geophys. Res.,* **109,** D07S90, doi:10.1029/2003JD003823.

Pampaloni, P., and S. Paloscia, 1986: Microwave emission and plant water content: A comparison between field measurements and theory. *IEEE Trans. Geosci. Remote Sens.,* **24,** 900–905.

Robock, A., K. Y. Vinnikov, G. Srinivasan, J. K. Entin, S. E. Hollinger, N. A. Speranskaya, S. Liu, and A. Namkhai, 2000: The Global Soil Moisture Data Bank. *Bull. Amer. Meteor. Soc.,* **81,** 1281–1299.

——, and Coauthors, 2003: Evaluation of the North American Land Data Assimilation System over the southern Great Plains during the warm season. *J. Geophys. Res.,* **108,** 8846, doi:10.1029/2002JD003245.

Rodell, M., B. F. Chao, A. Y. Au, J. S. Kimball, and K. C. McDonald, 2005: Global biomass variation and its geodynamic effects: 1982-1998. *Earth Interactions,* **9**. [Available online at http://EarthInteractions.org.]

Saleem, J. A., and G. D. Salvucci, 2002: Comparison of soil wetness indices for inducing functional similarity of hydrologic response across sites in Illinois. *J. Hydrometeor.,* **3,** 80–91.

Salvucci, G. D., 2001: Estimating the moisture dependence of root

zone water loss using conditionally averaged precipitation. *Water Resour. Res.,* **37,** 1357–1365.

——, J. A. Saleem, and R. Kaufmann, 2002: Investigating soil moisture feedbacks on precipitation with tests of Granger causality. *Adv. Water Resour.,* **25,** 1305–1312.

Schmugge, T. J., W. P. Kustas, J. C. Ritchie, T. J. Jackson, and A. Rango, 2002: Remote sensing in hydrology. *Adv. Water Resour.,* **25,** 1367–1385.

Seuffert, G., H. Wilker, P. Viterbo, M. Drusch, and J. F. Mahfouf, 2004: The usage of screen-level parameters and microwave brightness temperature for soil moisture analysis. *J. Hydrometeor.,* **5,** 516–531.

Tsang, L., J. A. Kong, E. Njoku, D. H. Staelin, and J. W. Waters, 1977: Theory for microwave thermal emission from a layer of cloud or rain. *IEEE Trans. Antennas Propag.,* **25,** 650–657.

Ulaby, F. T., M. Razani, and M. C. Dobson, 1983: Effects of vegetation cover on the microwave radiometric sensitivity to soil moisture. *IEEE Trans. Geosci. Remote Sens.,* **21,** 51–61.

——, R. K. Moore, and A. K. Fung, 1986: *From Theory to Applications*. Vol. 3, *Microwave Remote Sensing: Active and Passive*, Artech House, 1120 pp.

Zhang, T., R. L. Armstrong, and J. Smith, 2003: Investigation of the near-surface soil freeze-thaw cycle in the contiguous United States: Algorithm development and validation. *J. Geophys. Res.,* **108,** 8860, doi:10.1029/2003JD003530.